a reprint from Applied Optics

Ultrahigh-efficiency, very narrow-passband, tunable optical filter

Stephen P. Sandford and Milfred E. Thomas

Recently developed technologies have been uniquely integrated to produce optical filters with unprecedented performance. The precise design and fabrication of narrow-passband and high-efficiency optical filters with a central frequency of 532 nm are reported. Measurements with these filters demonstrate a performance that accurately mirrors the design specification, with one filter having a passband of 70 pm and an efficiency greater than 90% and the second filter having a passband of 7 pm and an efficiency greater than 80%.

Introduction

Optical filters with both narrow passbands and high efficiency can now be precisely fabricated to design specifications. These new filters offer tremendous improvements in the performance of a number of optical, infrared (IR), and photonic systems. These include fiber-optic[1] and space-based communications, where precise frequency discrimination will provide higher channel capacity. Active and passive remote sensors [e.g., NASA's LITE (Lidar In-Space Technology Experiment) and LASE (Lidar Atmospheric Sensing Experiment) lidar programs[2,3] and gas filter correlation radiometers] of small signal radiation against high-noise backgrounds will realize large gains in the signal-to-noise ratio (SNR) over the current state of the art because of increased signal and decreased noise at the detector. Finally, the size, weight, and power requirements of many optical and IR systems can be reduced by taking advantage of the gain in SNR that is delivered by optical bandpass filters with the performance characteristics described here.

Background

The designers of electronic measurement systems have long used the bandpass filter to improve the SNR in their measurements. Optical engineers have also tried to take advantage of techniques that remove all frequencies except those near the signal of interest to improve the SNR. However, until recently, optical bandpass filters presented the optical system designer with a difficult trade-off. The available filter technology (e.g., acousto-optic,[4] liquid crystal,[5] volume holographic,[6] and Fabry–Perot[7,8] filters) could provide narrow passbands but only with low efficiency. Similarly, high-efficiency filters could be built, but only by broadening of the passband (e.g., interference filters and Fabry–Perot étalons). Atomic line filters[9] provide both a narrow passband and good transmission but at the expense of size and complexity. Fabry–Perot devices were often used when efficiency was not critical and narrow passband was most important. Interference filters were used to maintain efficiency and still provide some degree of bandpass filtering.

The most recent developments in polishing techniques and in thin-film deposition permit the specification and fabrication of surfaces with well-known transmission coefficients and with extremely low losses A resulting from absorption and scattering (A is approximately 1 part in 10^6).[10] Improved polishing techniques permit rms surface roughnesses of less than 100 pm, which greatly reduces the losses that are due to stray reflections at the surface and provides an excellent interface for the first layer of the multilayer mirror coating. Furthermore, improved materials and coating-deposition techniques provide mirror coatings that are stoichiometrically homogeneous and have low stress interfaces between layers. Because maximum efficiency is determined by losses (efficiency $T/T + A$, where T is transmission), extremely high-efficiency surfaces can be built. This steep dependence of efficiency on A and T is illustrated in Fig. 1. When these surfaces are used

S. P. Sandford is with NASA Langley Research Center, Hampton, Virginia 23681. M. E. Thomas is with the Science and Technology Corporation, Hampton, Virginia 23681.

Received 19 November 1993; revised manuscript received 20 July 1994.

0003-6935/94/368325-05$06.00/0.

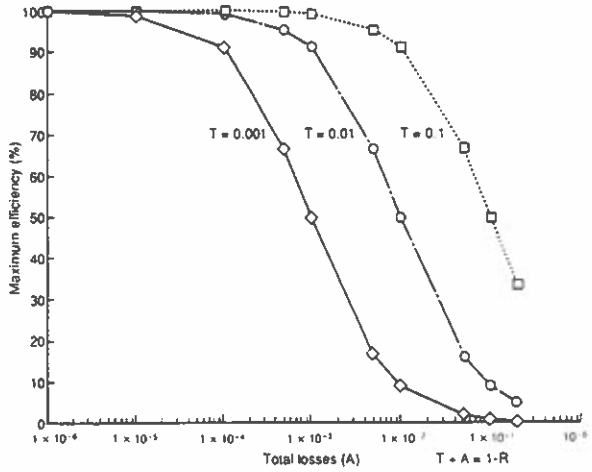

Fig. 1. Dependence of Fabry–Perot efficiency on losses (A) and transmission (T).

as mirrors in a Fabry–Perot configuration, both high efficiency and narrow passbands can be obtained simultaneously.

Another factor that is believed to increase the efficiency of these devices is the choice of a symmetric spherical geometry rather than the traditional plane–plane geometry. This reduces the mode size of the filter but also reduces the losses that are due to misalignment of the mirrors with respect to each other and of the filter with respect to the input beam.

The theory of the response and efficiency of Fabry–Perot filters is well documented.[11] Here this theory is assumed, and only the equations necessary for filter design are presented.

Design Analysis and Fabrication

Center Wavelength

The development of these particular filters came as the result of efforts to build smaller, less massive, and less expensive space-based atmospheric sensors. The filters were specifically designed for the first space-based lidar system.[2] In this lidar the channel with the most critical SNR detects the laser backscatter from the atmosphere at 532 nm, and the center wavelength of the filters discussed here was designed to be 532 nm. The exact center of the transmission curves for the mirrors fabricated was within 5 nm of this design specification, and the mirrors met the specification for transmission over a range of 10 nm (see Fig. 2).[12] This is important because it indicates that a designer can specify a particular center wavelength and be sure the manufacturer will deliver pieces that operate at that frequency.

Passband, Free Spectral Range, and Finesse

The next critical parameter in a filter design is the width of the passband. Ideally this width would correspond to that of the bandwidth of the signal to be measured. Doppler broadening and the linewidth of the LITE laser transmitter dictated a filter passband of 100 pm. The passband $\Delta\upsilon$ for a Fabry–Perot

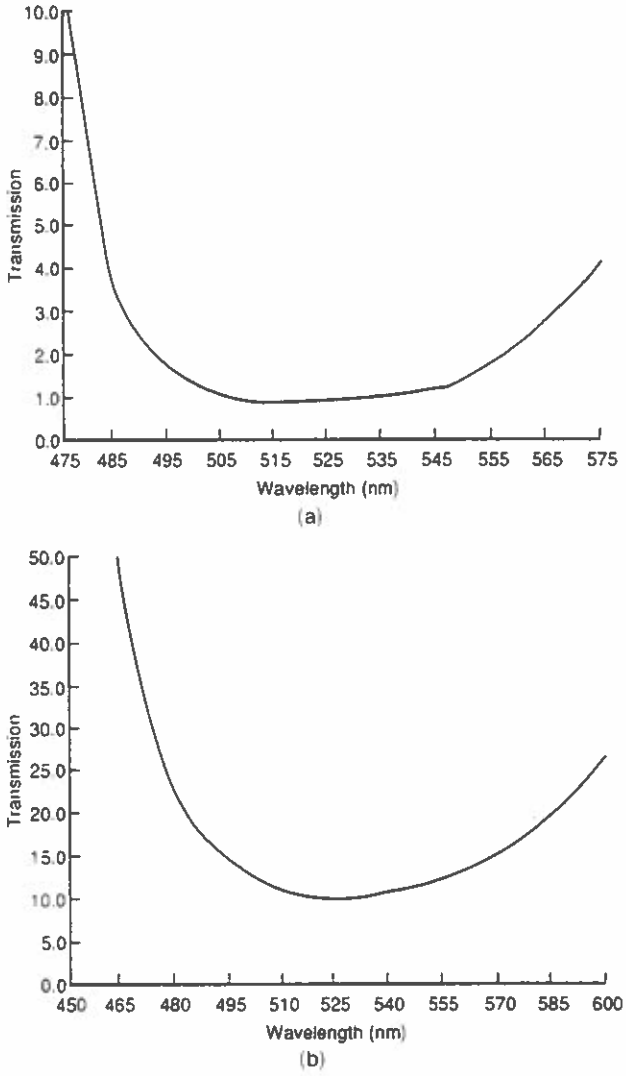

Fig. 2. Transmission response of mirrors in (a) 7-pm (b) 70-pm bandpass filters.

depends on two variables: the total finesse of the mirrors and the mirror spacing (L), which determines the free spectral range (FSR).

$$\Delta\upsilon = \mathrm{FSR}/\mathrm{finesse}, \tag{1}$$

where the FSR is $c/2L$ and c is the speed of light. Because a Fabry–Perot cavity resonates at a large number of frequencies, each separated by the FSR, it must be placed in series with a broadband filter to remove all frequencies but those in the narrow band of interest. It is critical that this second filter not destroy the gain in efficiency of the new Fabry–Perot filter. However, as noted above, high efficiency may be obtained for interference filters as long as the passband is wide enough. This fact and the $1/L$ dependence of the FSR dictate a small spacing between the mirrors to provide a large FSR, thus permitting the use of wide-passband interference filters to remove other harmonics. In this design $L = 100\ \mu\mathrm{m}$, which gives us a FSR of 1.5 THz, or 1400 pm (see Fig. 3). Equation (1) then permits the

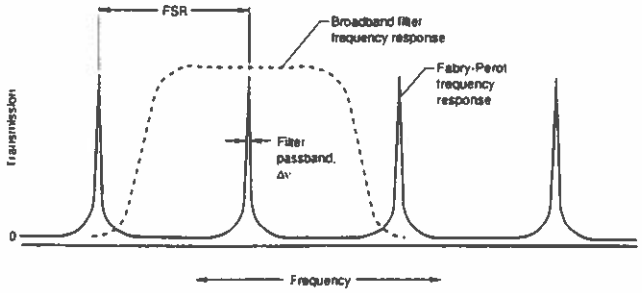

Fig. 3. Frequency response of elements required for narrow-passband receiver filter.

determination of the mirror finesse that is required to achieve the desired passband.

When the mirrors for these filters were fabricated, the finesse was specified to be 15 for a passband of 100 pm and 150 for a passband of 10 pm. More specifically the coating producer needs to know the reflectivity R for each mirror. Because the polish or superpolish on the mirror surfaces is less than 100 pm rms surface roughness, the total finesse is given by the reflectivity finesse, which depends on only R. The finesse can be related to the mirror reflectivity with the Airy formula for transmission through a multilayer interface[13]:

$$\frac{I(t)}{I(i)} = \frac{1}{1 + F \sin^2(d/2)}, \tag{2}$$

where d is the phase that is accumulated in one round-trip through the interface (in this case the filter) and $F = 4R/(1 - R)^2$ is the coefficient of finesse, if high-reflectivity surfaces are assumed. For the intensity at half the maximum in the passband, the condition for resonance yields

$$d/2 = m\pi \pm \Delta\upsilon/4. \tag{3}$$

For narrow-passband filters where the fringes are sharp, one can assume that $\Delta\upsilon$ is small and use the small-angle approximation to write

$$\frac{I(t)}{I(i)} = \frac{1}{2} = \frac{1}{1 + F \sin^2(\Delta\upsilon/4)} = \frac{1}{1 + F(\Delta\upsilon/4)^2}. \tag{4}$$

Solving for $\Delta\upsilon$ yields

$$\Delta\upsilon = 4/\sqrt{F}. \tag{5}$$

The definition of finesse[14] is the ratio of the separation between the fringes and the passband of each fringe, and therefore

$$\text{finesse} = \pi/\Delta\upsilon = (\pi\sqrt{R}/2(1 - R). \tag{6}$$

Thus, for a finesse of 15, $R = 0.90$, and for a finesse of 150, $R = 0.99$. As can be seen in Fig. 1, the optical filter designer can expect excellent agreement between the specification and the manufactured mirror performance in both the center frequency and reflectivity and the transmission coefficients that determine the passband width.

Alignment and Mode Matching

Another important criterion in this design for a space-based lidar receiver filter is ease of alignment and mode matching.[15] To design a resonator so that the mode matching and alignment of the mirrors to each other is simple, a confocal design would be chosen. However, a practical confocal design, because of the large mirror sag, would yield a FSR that is too small to maintain high efficiency, as discussed above. The plane–plane configuration also makes mode matching easy because all the modes are degenerate; however, this forces the unwanted constraint of high parallelism between the mirrors. Thus the compromise that was chosen for this design was to make the mirrors with a spherical radius of curvature r of 10 m. This selection determines the mode size, a critical parameter, which yields the transverse dimension of the beam when it enters the resonator. Energy outside of this diameter will not resonate and will contribute to the total loss of the filter. The mode size b for a symmetric spherical mirror resonator is given by the equations for Gaussian beam propagation,[16] which when combined yield the approximate expression

$$\text{mode size} = b^2 \approx \lambda\sqrt{rL/2}. \tag{7}$$

For the filters described here the mode diameter was approximately 110 μm. The cavity mirror radius of curvature and spacing also determines the distance between transverse modes. This mode spacing is given by the following relation[17]:

$$\text{transverse mode spacing} = \frac{c}{2L}\frac{\cos^{-1} g}{\pi}. \tag{8}$$

The cavity parameter g (Ref. 18) depends on the mirror spacing and the radius of curvature, with $g = 1 - L/r$. The mode spacing should be small relative to the passband width to reduce the sensitivity of the filter linewidth to alignment, because the power in the transverse modes is a function of alignment. Specifically the transverse modes should all lie within the filter passband. For these filters the design passbands were 100 GHz (100 pm) and 10 GHz (10 pm), and the mode spacing was 2 GHz.

Experiment Setup

The experiment setup (see Fig. 4) was designed to demonstrate that the latest polishing and coating technology permits the specification and fabrication of mirrors that are useful for the construction of a narrow-passband and high-efficiency Fabry–Perot optical filter. The setup design concentrates on measurements of efficiency and passband width. The passband width depends on the FSR so the setup permits the measurement of the spacing L between the mirrors. This distance was measured with a United Detector Technologies UDT 531 position sen-

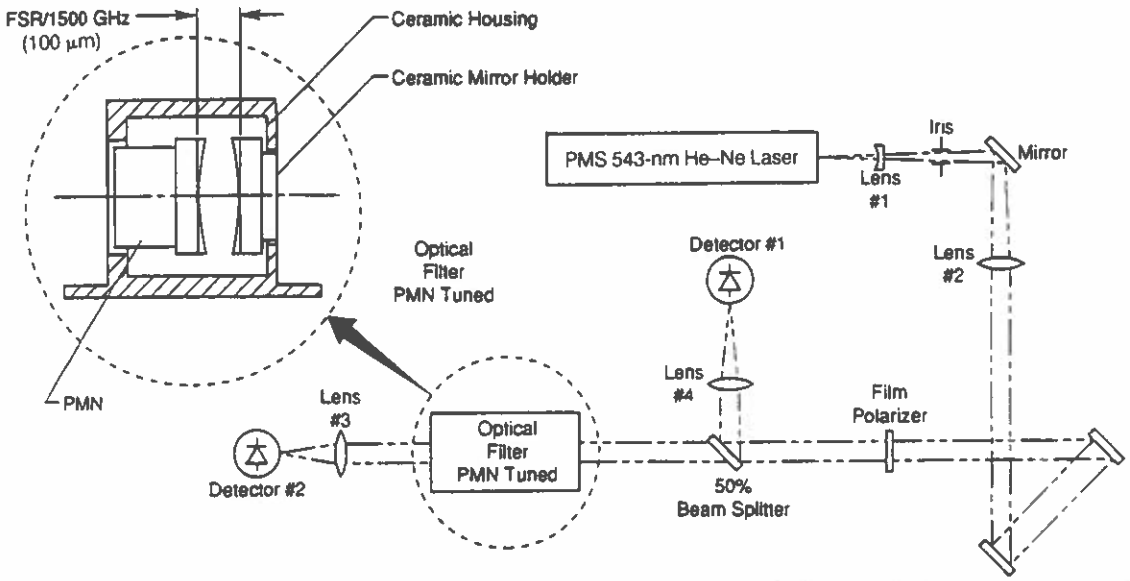

Fig. 4. Experiment schematic. PMN, electrostrictive material composed of lead (Pb), magnesium (Mg), and niobate (N).

sor and lateral-effect diode detectors. We measured the efficiency by splitting the beam and sending exactly half the power to the filter and half to an identical reference photodetector. The ratio of the power transmitted through the filter to the power in the reference detector is the efficiency. We measure the passband width by sweeping the filter center frequency over at least one FSR and displaying the transmitted power on an oscilloscope triggered by the triangle-wave-sweep voltage. The distance between the mirrors yields the FSR in hertz and therefore allows us to calibrate the oscilloscope time base (i.e., the number of hertz per millisecond). The full-width at half-maximum can then be measured with an accuracy that is limited by the uncertainty in the measurement of mirror spacing.

Experimental Results

Two separate filters were designed and built. They were designed with passbands of 100 and 10 pm, respectively. As stated above, this design translates into mirror reflectivities of 0.90 and 0.99, respectively. The mirror spacing was set to 100 μm, yielding a FSR of 1.5 nm, which would permit an interference filter with a 3-nm passband, and thus with high efficiency, to be used in series with the Fabry–Perot filter. The measured passbands were 70 and 7 pm for the two filters. The transmission efficiencies measured were greater than 90% and greater than 80%, respectively. The difference between the design and the actual passband widths is due to two factors. The first is that the laser used to make the measurements was centered at 543 nm instead of the design center wavelength of 532 nm. The error as a result of this difference in center wavelength is 15% and is determined with Fig. 2 and Eq. (6), which relates finesse to reflectivity. The second source of error is the measurement of FSR. The error here is due to uncertainty in the mirror sag, in the distance between the mirrors themselves, and in the oscilloscope reading. The total measurement error here is also 15%. The 30% difference between the design and the measured passband therefore primarily is due to the center wavelength of the laser used in the measurement and to errors in establishing the 100-μm mirror spacing. Figure 5 is a typical oscilloscope trace that shows the filter transmission as the filter center frequency is scanned over a FSR.

The plot shown in Fig. 5 was taken with the 7-pm filter. The small asymmetry visible at the base of each line is due to high-order transverse-mode frequencies outside the axial-mode passband. This asymmetry can be remedied by reduction of the transverse-mode separation. Increasing L to reduce this separation will also decrease the FSR and increase the mode size.

It is recommended that the radius of curvature be increased from 10 m to between 50 and 100 m to

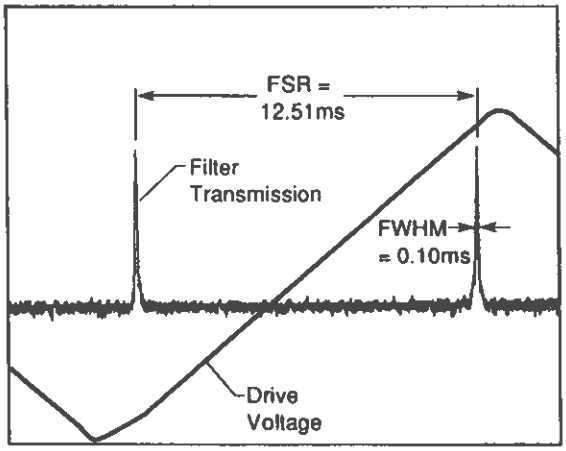

Fig. 5. Filter transmission versus frequency. Tuning over a FSR allows us to calibrate the oscilloscope time base.

increase the mode size without sacrificing ease of alignment or walk-off losses.

Conclusions

Optical engineers no longer must face the trade-off between narrow-bandpass filtering and loss of signal in the design of optical and IR signal-processing and detection systems. Polishing and coating techniques have evolved to the point that a narrow passband can be accompanied by high efficiency. Specifically, an optical filter with a 7-pm passband and over 80% efficiency has been demonstrated. A 70-pm passband filter has over 90% efficiency. This combination of narrow passband and high efficiency is available because of the extremely low losses in the mirrors as a result of absorption and scattering. Losses are further reduced and alignment is eased by the use of a symmetric spherical Fabry–Perot configuration.

These narrow passbands will improve performance in most remote-sensing applications because the spectral features that are being measured are broader than these passbands. In addition, the sharp frequency discrimination that these filters deliver will increase the information-carrying capacity of optical communication channels in both fiber-optic and space-based communication systems. As frequency-controlled lasers become more prevalent these novel, high-efficiency, narrow-passband filters will make an even larger impact on optical system design.

The Flight Electronics Division at NASA Langley Research Center supported this work entirely with discretionary funding. Bill Stevens built the filter scanning electronics that were used to make the passband measurements. Duane Willis and Ramin Lalezari at PMS Research Electro-Optics, Boulder, Colorado, are responsible for the high quality of the mirrors used in these Fabry–Perot filters.

References and Notes

1. R. Boucher, B. Villeneuve, M. Breton, and M. Tetu, "Calibrated Fabry–Perot etalon as an absolute frequency reference for OFDM communications," Photon. Technol. Lett. **4,** 801–804 (1992).
2. R. H. Couch, C. W. Rowland, K. S. Ellis, M. P. Blythe, C. P. Regan, M. R. Koch, C. W. Antill, W. L. Kitchen, J. W. Cox, J. F. DeLorme, S. K. Crockett, R. W. Remus, J. C. Casas, and W. H. Hunt, "LIDAR In-space Technology Experiment (LITE): NASA's first in-space LIDAR system for atmospheric research," Opt. Eng. **30,** 88–95 (1991).
3. W. R. Vaughan and E. V. Browell, "A LIDAR instrument to measure H_2O and aerosol profiles from the NASA ER-2 aircraft," presented at the Specialty Meeting on Airborne Radars and Lidars, Meteo-France, Toulouse, France, 7–10 July 1992.
4. I. C. Chang, "Acousto-optic tunable filters," Opt. Eng. **20,** 824–829 (1981).
5. K. Hirabayashi, H. Tsuda, and T. Kurokawa, "Tunable wavelength-selective liquid crystal filters for 600-channel FDM system," Photon. Technol. Lett. **4,** 597–599 (1992).
6. G. A. Raukuljic and V. Leyva, "Volume holographic narrowband filter," Opt. Lett. **18,** 459–461 (1993).
7. K. Hsu and C. Miller, "Stretching fiber's ability to look at light," Photon. Spectra **27**(5), 135–136 (1993).
8. A. K. Jain, D. E. Stoltzmann, G. R. Knowles, J. G. Droessler, and D. Johnson, "Dual tunable Fabry–Perot spectrally tunable agile filter," Opt. Eng. **23,** 159–166 (1984).
9. J. Alvarez, L. M. Caldwell, Y. H. Li, D. A. Krueger, and C. Y. She, "High-spectral resolution lidar measurement of tropospheric backscatter ratio using barium atomic blocking filters," J. Atmos. Oceanic Technol. **7,** 876–881 (1990).
10. R. Lalezari, PMS Research Electro-Optics, Boulder, Colo. 80306 (personal communication, May, 1992).
11. P. D. Atherton, N. K. Reay, J. Ring, and T. R. Hicks, "Tunable Fabry–Perot filters," Opt. Eng. **20,** 806–814 (1981).
12. The transmission curves are courtesy of PMS Research Electro-Optics, and they give the performance of the mirrors used in the experiments described in this paper. PMS is also responsible for the mirror substrate polishing.
13. D. Winker, Atmospheric Sciences Division, NASA Langley Research Center, Hampton, Va. 23681 (personal communication, January, 1992).
14. M. Born and E. Wolf, *Principles of Optics* (Pergamon, New York, 1987), Chap. 7, pp. 323–329.
15. J. Wyant, University of Arizona, Tucson, Ariz. 85726 (personal communication, March, 1989).
16. H. Kogelnik and T. Li, "Laser beams and resonators," Proc. Inst. Electr. Eng. **54,** 1550–1567 (1966).
17. J. D. Gaskill, *Linear Systems, Fourier Transforms, and Optics* (Wiley, New York, 1978), Chap. 10, pp. 420–435.
18. A. E. Siegman, *Lasers* (University Science, Mill Valley, Calif., 1986), Chap. 19, pp. 744–748.